Journal of Engineering Research (ERJ)
Vol. 7 – No. 2, 2023
©Tanta University, Faculty of Engineering
https://erjeng.journals.ekb.eg/
ISSN: 2356-9441
e ISSN: 2735-4873

Investigation of Some Physical Properties of the Nanosized ZnO Prepared by the Coprecipitation Method

N. Asal[1], S.T. Assar[2,*], B.M. Mohrram[3], O. Hatem[2]

[1] M. Sc. Student, Engineering Physics and Mathematics Department, Faculty of Engineering, Tanta University, Tanta, Egypt
[2]Assoc. Professor, Engineering Physics and Mathematics Department, Faculty of Engineering, Tanta University, Tanta, Egypt
[3]Professor, Engineering Physics and Mathematics Department, Faculty of Engineering, Tanta University, Tanta, Egypt
[*]Corresponding author: s_talaat@f-eng.tanta.edu.eg, email: nadiaasal@f-eng.tanta.edu.eg, s_talaat@f-eng.tanta.edu.eg, bahaa.mouharam@f-eng.tanta.edu.eg, osama.hatem@f-eng.tanta.edu.eg

***Abstract*-Zinc oxide (ZnO) nanoparticles have been fabricated via the coprecipitation method, where their structural, magnetic, and thermal features have been scrutinized in tandem with their optical peculiarities. The structural characteristics have been inspected through the X-ray diffraction patterns, particle size distribution, "transmission electron microscopy TEM," BET analysis, and "Fourier transform Infrared spectroscopy FTIR," which confirm the nanostructure of the ZnO particles. The BET analysis confirms the mesoporous nature of the ZnO nanoparticles. The magnetic properties have been investigated by the "vibrating sample magnetometer VSM". The hysteresis (M-H) loop ensures the paramagnetic behavior of the ZnO nanoparticles. The measured thermal conductivity of the ZnO equals 0.2901 W/mK. The very low thermal conductivity value for the ZnO nanoparticles makes it an attractive contender for thermoelectric power applications. UV-vis Diffuse reflectance spectroscopy has been exploited to study the optical properties. The nano ZnO direct and indirect band gap energy determined using Tauc's relation are 3.29 and 3.09 eV, respectively. The optical properties, high porosity, and specific surface area of the prepared nanosized ZnO particles make it a promising candidate for photocatalytic application.**

***Keywords*-ZnO nanoparticles, BET analysis, Magnetic properties, UV-vis DRS, thermal conductivity.**

I. INTRODUCTION

Recently, metal oxides characterized by distinctive magnetic, ferroelectric, dielectric, conductive, and optical peculiarities have allured considerable attentiveness to be utilized in various device applications. The considerably broad bandgap (3.37 eV), high exciton binding energy (60 meV), and high electron mobility of zinc oxide (ZnO) have made it a popular metal oxide in recent years [1]. It is widely employed in many applications, such as solar cells, photocatalysts, field-effect transistors, light-emitting diodes, sensors, etc. It is also considered an II-VI n-type semiconductor crystalline material, and it can be found in three different phases, including wurtzite, rock salt, and zinc blend. Due to its ionicity being precisely at the boundary between covalent and ionic materials, wurtzite is more immutable than other phases.

One of the reported potential thermoelectric materials is zinc oxide (ZnO). It exhibits exceptional mechanical, thermal, and chemical immutability, corrosion resistance, degradability, and ease of production and doping. Moreover, ZnO is an affordable, safe, and low-toxic substance. As mentioned before, thermoelectric materials are of great importance, so in this work, nanoparticles of ZnO which are promising thermoelectric candidates with an extremely low thermal conductivity than reported, have been fabricated

II. EXPERIMENTAL TECHNIQUES

A. *Preparation of nanocrystalline ZnO*

The chemical co-precipitation approach, frequently employed due to its simplicity and effective control over grain size, was utilized to create the nanostructure ZnO sample. In this method, the desired amounts, according to the stoichiometric ratio, of $Zn(NO_3).6H_2O$ and NaOH were weighed and dissolved independently in distilled water. Then, the zinc nitrate solution was stirred continuously for around 15 minutes before adding the sodium hydroxide solution dropwise to it till the pH of the mixture reached 13. After then, the mixture was left at 90 °C for an hour to consummate the reaction. Finally, the resulting precipitates were washed several times to remove unwanted contaminants before being dried for 24 hours in a drying oven at 80°C and pulverized into a fine powder. The steps of the nano ZnO sample are shown in Fig. 1.

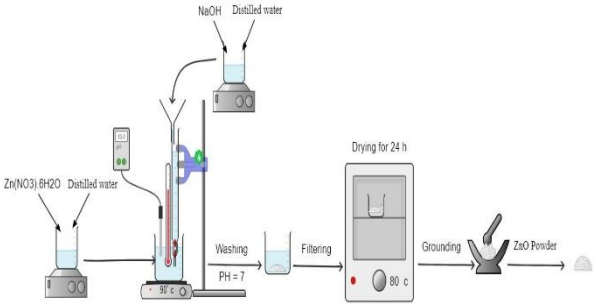

Figure 1: The preparation steps of ZnO nanoparticles.

B. *Characterization techniques*

X-ray Diffraction (XRD) model "XPERT- PRO-PANalytical-Netherland" was used to assess the sample's structure at room temperature RT. The target was CuK, and the incident radiation's wavelength was 1.5406 Å. Using the instrument's software "XRD Panalytical X'PERT PRO," the average crystallite size D_{311} of the sample was calculated from the full width at half maximum (FWHM) of the strongest reflection of the plane (311). Depending on the Williamson-Hall approach, the above software evaluated the microstrain

DOI: 10.21608/ERJENG.2023.204295.1171

Journal of Engineering Research (ERJ)
Vol. 7 – No. 2, 2023
©Tanta University, Faculty of Engineering
https://erjeng.journals.ekb.eg/
ISSN: 2356-9441
e ISSN: 2735-4873

and average crystallite size [23]. Instrumental broadening corrections have been made using an X-ray profile fitting of highly crystalline standard reference material (Silicon SRM 640e approved by NIST) in order to eliminate the measuring inaccuracies brought on by the instrument. Together with illustrating the particle size distribution (PSD) in the sample, the particle size analyzer PSA model "BECKMAN COULTER" has also been utilized to examine the nanostructure of the sample and determine its average particle sizes. The laser beam's incidence angles have been measured at two different angles (10.9º and 15.4º). The specifics of this measurement have already been covered [6]. The (FTIR) spectra were captured using the "Bruker FT-IR TENSOR 27"- with a resolution of 4 cm^{-1} and a wave number range of 200 to 4000 cm^{-1}.

Additionally, using the "Lake Shore 7410 model" VSM with a maximum applied magnetic field of about 20 kG, measurements of the sample's M-H loop and magnetization have been made at RT. Thermal properties of the sample, including thermal conductivity K_s, thermal diffusivity α_s, and specific heat capacity C_p, were obtained using a constant thermal analyzer "Hot Disk TPS 500". UV-vis DRS was used to determine the bandgap energy of the prepared ZnO sample by the "V-700 UV/VIS/NIR" spectrophotometer.

III. RESULTS AND DISCUSSION

A. Structural Analysis

The XRD patterns show some well-defined peaks at Miller Indices (1100, 2002, 3101, 4102, 5110, 6103, 8112), as manifested in Fig. 2, that support the development of hexagonal close packing (HCP) wurtzite ZnO that belongs to space group P63mc. Table. 1 shows the structural parameters *a* and c, crystallite size D_{XRD}, x-ray density ρ_x, measured density ρ_m, porosity *P* as well as the specific surface area *S*, and microstrain η. These structural characteristics were computed using the relationships made clear in earlier research work [2].

The structural parameters *a* and *c* of the HCP of the ZnO are calculated using the Miller Indices (h, k, l) of the XRD high-intensity peaks and the corresponding *d*-spacing according to the following equation [3]:

$$\frac{1}{d^2} = \frac{3}{4}\left(\frac{h^2+hk+k^2}{a^2}\right) + \frac{l^2}{c^2} = \frac{4(\sin\theta)^2}{\lambda^2} \quad (1)$$

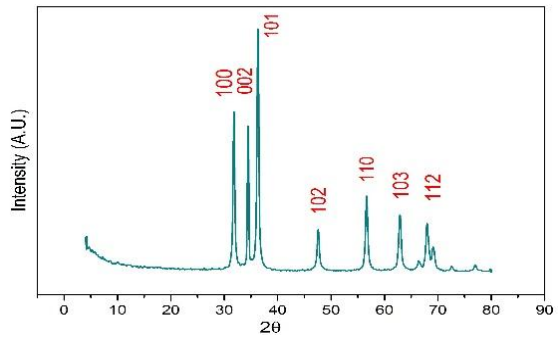

Figure 2: The XRD pattern of the prepared ZnO nanoparticles

Table 1: The structural parameters of the ZnO nanoparticles.

Sample	*a* Å	*c* Å	D_{XRD} *nm*	ρ_x g/cm^3	ρ_m g/cm^3	*P* %	*S* m^2/g	*η* %
ZnO	3.25	5.207	21.6	5.68	2.6	52	49	0.6

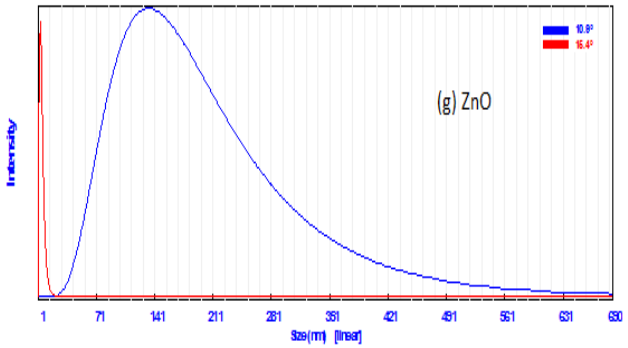

Figure 3: the PSD of the ZnO nanoparticles.

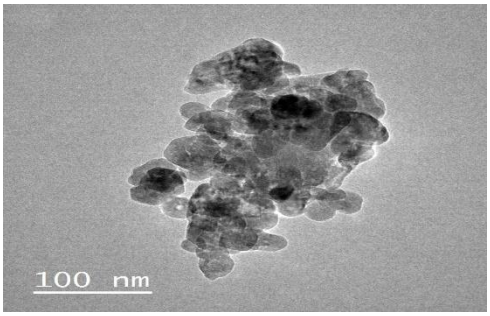

Figure 4: TEM image of the prepared ZnO nanoparticles.

Table 2: PSD and TEM size of the sample.

Sample	D_{MAX} *(nm)*		D_{PSA} *(nm)*	D_{TEM} *(nm)*
	θ_i*=10.9º*	θ_i*=15.4º*	*average*	*average*
ZnO	131	3.7	67.35	39.8

The existence of non-uniform lattice distortions, faulting, dislocations, antiphase domain borders, grain surface relaxation, and solid solution inhomogeneity as causes of microstrain are well documented in the literature. The examined samples' positive values reveal the tensile strain in their crystal lattices [4], [5].

Fig. 3 demonstrates the PSD of the prepared ZnO sample, recorded at two angles of 10.91o and 15.41o, as mentioned above. Meanwhile, Table 2 shows the DMAX value at both measured angles and the resultant average particle sizes D_{PSA}. The obtained result confirms the nano nature of the prepared ZnO.

The agglomerated irregular-shaped ZnO nanoparticles are observed in Fig. 4, while Table 2 displays the ZnO's average particle size D_{TEM}, determined using the Image J software program. The D_{TEM} value agrees with that previously obtained through the PSD and XRD results.

The hysteresis loop of the adsorption-desorption for the ZnO is shown in Fig. 5, and the obtained parameters are

DOI: 10.21608/ERJENG.2023.204295.1171

Journal of Engineering Research (ERJ)
Vol. 7 – No. 2, 2023
©Tanta University, Faculty of Engineering
https://erjeng.journals.ekb.eg/
ISSN: 2356-9441
e ISSN: 2735-4873

tabulated in Table 3, where the mesoporous nature of the ZnO nanoparticles is confirmed. Also, the FTIR spectrum of ZnO is shown in Fig. 6, where a broad, intense peak is noticed at v_2 = 406 cm^{-1}, allocated to the Zn-O bond's stretching vibrations [6].

Table 3: BET parameters of ZnO.

Sample	S_{BET} (m^2/g)	*Pore diameter (nm)*	*Pore size×10^{-2} (cm^3/g)*	*Porosity %*
ZnO	11.52	32.131	9.25	53

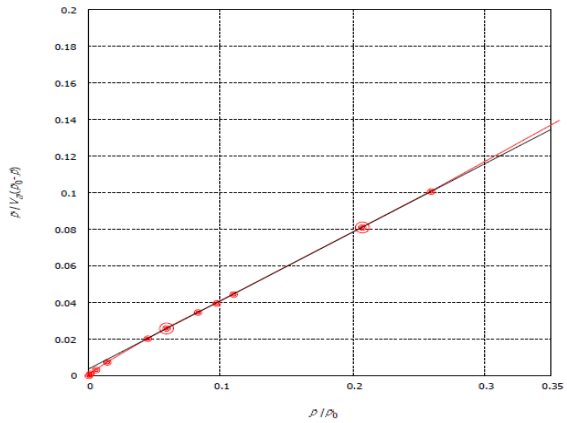

Figure 5: BET hysteresis loop of the ZnO nanoparticles

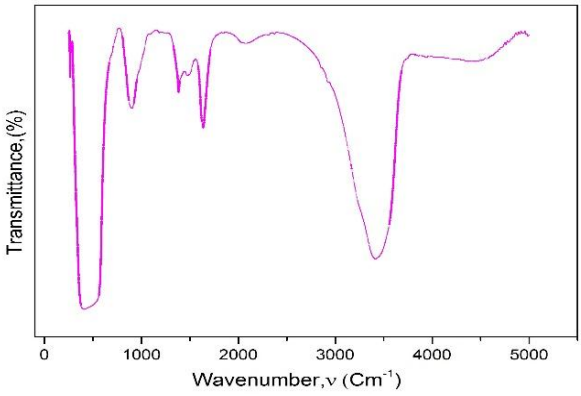

Figure 6: FTIR spectrum of the ZnO nanoparticles.

Table 4: The IR-deduced parameters

Sample	v_3 cm^{-1}	v_2 cm^{-1}	v_{th} cm^{-1}	E_{th} *eV*	*J(×10^{13}) Hz*
ZnO	255	406	774	0.0962	2.60

Moreover, this spectrum is exploited in obtaining the intrinsic lattice vibration v_1, in addition to the threshold wavenumber and the threshold energy of electron transition, calculated by the equation mentioned in the following reference [7]. Also, the charge carrier's jump rate J for migration between lattice vacancies is listed in Table 4.

Table 5: The VSM-deduced parameters

Sample	M_s *emu/g*	H_c *G*	M_r *emu/g*	K_1 *erg/G*	*Ls Erg/g*	S_q M_r/M_s
ZnO	0.023	150	0.0003	4	8.94	0.015

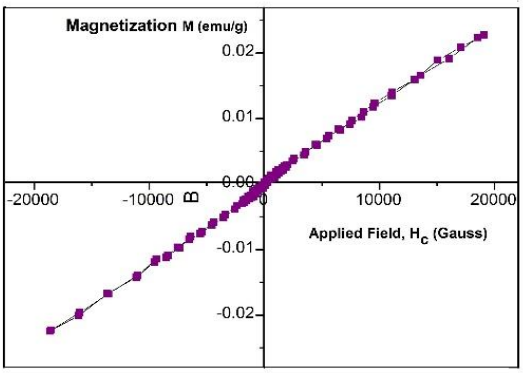

Figure 7: VSM loop of the ZnO nanoparticles

B. *Magnetic Properties*

The room temperature hysteresis loop of the nano ZnO is presented in Fig. 7, and its magnetic properties are listed in Table 5. The sample demonstrates paramagnetic behavior with considerably small saturation M_s and remanent M_r magnetization. Besides, low coercivity, magnetic losses L_s, and squareness S_q are detected.

Grain size, measured density, porosity, strain, morphology, saturation magnetization, and magneto-crystalline anisotropy are the competing elements that influence the behavior of H_c [8]–[10]. The following equation relates the final two elements to coercivity [11]:

$$H_c = \frac{0.96K_1}{M_S} \quad (2)$$

C. *Thermal Properties*

Designing a range of microwave devices that operate at high power levels requires understanding the thermal properties of metal oxide materials. These characteristics include α_s, K_s, and C_p. The equation in the following reference [12] establishes a correlation between these thermal characteristics.

Compared to the values reported in the literature (6.0W/mK) by Correia et al. [1] and (49.0W/mK) by Sulaiman et al. [13], ZnO demonstrates poor thermal conductivity. It is important to note that one of the main challenges to ZnO's use in thermoelectric applications is its high thermal conductivity. The findings of this study (see Table. 6) refer that the prepared ZnO nanoparticles have the potential to get around this problem, making ZnO an attractive contender for various uses.

Table 6: The thermal parameters of the sample.

Sample	K_s *(W/mK)*	α_s *(mm²/s)*	C_p *(MJ/m³K)*
ZnO	0.2901	0.3720	0.7798

DOI: 10.21608/ERJENG.2023.204295.1171

Journal of Engineering Research (ERJ)
Vol. 7 – No. 2, 2023
©Tanta University, Faculty of Engineering
https://erjeng.journals.ekb.eg/
ISSN: 2356-9441
e ISSN: 2735-4873

Table 7: The optical parameters of the ZnO nanoparticles

Sample	*λ (nm)*	*Direct E_g (eV)*	*Indirect E_g (eV)*
ZnO	348	3.27	3.09

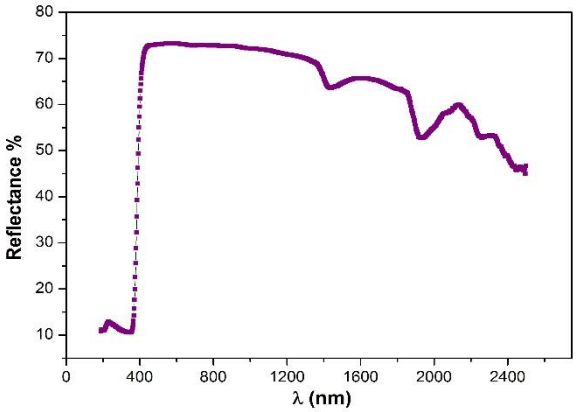

Figure 8: The DRS of the ZnO nanoparticles.

D. *Optical Properties*

The optical characteristics of the produced ZnO nanoparticles were examined using UV-vis diffuse reflectance spectroscopy recorded across the scope of 190-2500 nm at room temperature. The DRS is preferable to UV-vis absorbance spectroscopy for analyzing powdered samples because it causes less scattering [14]. The sample's UV-vis diffused reflection spectra are shown in Fig. 8, and the sample's measured reflection band ranges from 212 to 441 nm, as indicated in Table 7.

Moreover, using the spectrum data, the nano ZnO direct and indirect band gap energy, which were determined using Tauc's relation [15], are displayed in Table 7. The values of its direct and indirect band gap energy are coincidental with the values reported in the literature [16], [17]. Taucs plots for the direct and indirect bandgap are illustrated in Fig. 9 (a and b).

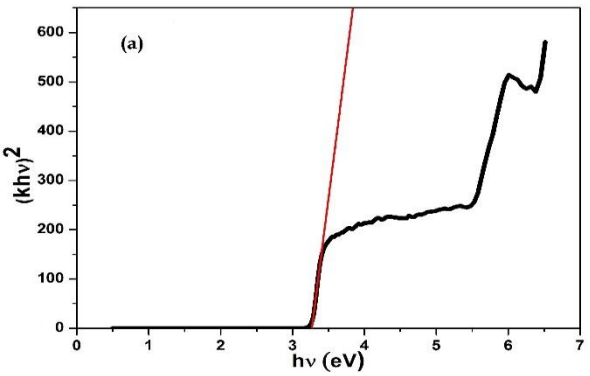

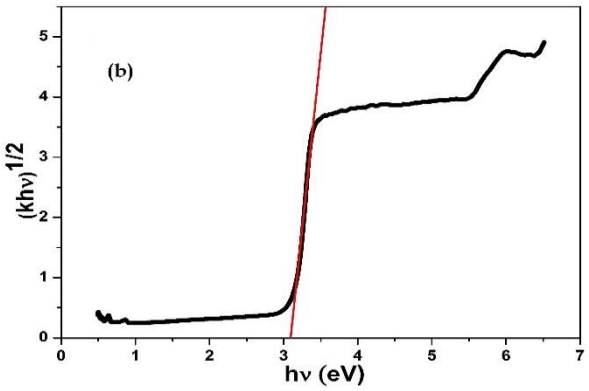

Figure 9: (a) direct bandgap and (b) the indirect band gap Taucs plot.

IV. CONCLUSION

Nano ZnO has been synthesized via the coprecipitation method. The prepared sample demonstrated nano-size nature according to the XRD, PSD, and TEM. Also, the BET analysis confirmed that ZnO has mesoporous particles. The VSM confirmed the paramagnetic behavior of the prepared ZnO. Moreover, the thermal properties reward the validity of the prepared ZnO for being utilized in thermoelectric applications due to its remarkably low thermal conductivity. Finally, the band gap of the produced ZnO nanoparticles agreed with the reported value in the literature, which makes it a viable choice as a photocatalytic material for pollutant degradation due to its optical characteristics, high porosity, and specific surface area.

Funding: The authors should mention if this research has received any type of funding.

Conflicts of Interest: The authors should explicitly declare if there is a conflict of interest.

REFERENCES

[1] F. C. Correia *et al.*, "The effect of Bi doping on the thermal conductivity of ZnO and ZnO:Al thin films," *Vacuum*, vol. 207, no. October 2022, pp. 1–7, 2023, doi: 10.1016/j.vacuum.2022.111572.

[2] S. Debnath, K. Deb, B. Saha, and R. Das, "X-ray diffraction analysis for the determination of elastic properties of zinc-doped manganese spinel ferrite nanocrystals (Mn0.75Zn0.25Fe2O4), along with the determination of ionic radii, bond lengths, and hopping lengths," J. Phys. Chem. Solids, vol. 134, no. July 2018, pp. 105–114, 2019, doi: 10.1016/j.jpcs.2019.05.047.

[3] A. S. Hamed, I. A. Ali, M. El Ghazaly, M. Al-abyad, and H. E. Hassan, "Physica B : Physics of Condensed Matter Nanocomposites of ZnO mixed with different Ni-ferrite contents : Structural and magnetic properties," Phys. B Phys. Condens. Matter, vol. 607, no. October 2020, p. 412861, 2021, doi: 10.1016/j.physb.2021.412861.

[4] S. T. Assar, H. F. Abosheiasha, and A. R. El Sayed, "Effect of γ-rays irradiation on the structural, magnetic, and electrical properties of Mg–Cu–Zn and Ni–Cu–Zn ferrites," J. Magn. Magn. Mater., vol. 421, pp. 355–367, 2017, doi: 10.1016/j.jmmm.2016.08.028.

[5] P. Thakur, R. Sharma, V. Sharma, and P. Sharma, "Structural and optical properties of Mn0.5Zn0.5Fe2O4 nano ferrites: Effect of sintering temperature," Mater. Chem. Phys., vol. 193, pp. 285–289, 2017, doi: 10.1016/j.matchemphys.2017.02.043.

[6] B. Karthikeyan, T. Pandiyarajan, and K. Mangaiyarkarasi, "Optical properties of sol-gel synthesized calcium doped ZnO nanostructures,"

ISSN: 2356-9441
e ISSN: 2735-4873

Spectrochim. Acta - Part A Mol. Biomol. Spectrosc., vol. 82, no. 1, pp. 97–101, 2011, doi: 10.1016/j.saa.2011.07.005.

[7] R. E. El-Shater, H. El Shimy, and S. T. Assar, "Investigation of physical properties of synthesized Zr doped Ni–Zn ferrites," Mater. Chem. Phys., vol. 247, no. January, p. 122758, 2020, doi: 10.1016/j.matchemphys.2020.122758.

[8] R. R. Kanna, N. Lenin, K. Sakthipandi, and A. S. Kumar, "Structural, optical, dielectric and magnetic studies of gadolinium-added Mn-Cu nanoferrites," J. Magn. Magn. Mater., vol. 453, pp. 78–90, 2018, doi: 10.1016/j.jmmm.2018.01.019.

[9] M. N. Akhtar, M. S. Nazir, Z. Tahir, S. Qamar, and M. A. Khan, "Impact of Co doping on physical, structural, microstructural and magnetic features of MgZn nanoferrites for high frequency applications," Ceram. Int., vol. 46, no. 2, pp. 1750–1759, 2020, doi: 10.1016/j.ceramint.2019.09.149.

[10] G. Lal et al., "Exploring the structural, elastic, optical, dielectric and magnetic characteristics of Ca2+ incorporated superparamagnetic Zn0.5−xCa0.1Co0.4+xFe2O4 (x = 0.0, 0.05 & 0.1) nanoferrites," J. Alloys Compd., vol. 886, p. 161190, 2021, doi: 10.1016/j.jallcom.2021.161190.

[11] E. F. Attia, A. H. Zaki, S. I. El-Dek, and A. A. Farghali, "Synthesis, physicochemical properties and photocatalytic activity of nanosized Mg doped Mn ferrite," J. Mol. Liq., vol. 231, pp. 589–596, 2017, doi: 10.1016/j.molliq.2017.01.108.

[12] H. F. Abosheiasha, and S. T. Assar, "Synthesis and study the physical properties of the nanosized," J. Mol. Struct., vol. 1166, pp. 334–343, 2018, doi: 10.1016/j.molstruc.2018.04.041.

[13] S. Sulaiman, S. Izman, M. B. Uday, and M. F. Omar, "Review on grain size effects on thermal conductivity in ZnO thermoelectric materials," RSC Adv., vol. 12, no. 9, pp. 5428–5438, 2022, doi: 10.1039/d1ra06133j.

[14] S. Debnath and R. Das, "Study of the optical properties of Zn doped Mn spinel ferrite nanocrystals shows multiple emission peaks in the visible range –a promising soft ferrite nanomaterial for deep blue LED," J. Mol. Struct., vol. 1199, p. 127044, 2020, doi: 10.1016/j.molstruc.2019.127044.

[15] P. Thakur, D. Chahar, S. Taneja, N. Bhalla, and A. Thakur, "A review on MnZn ferrites: Synthesis, characterization and applications," Ceram. Int., vol. 46, no. 10, pp. 15740–15763, 2020, doi: 10.1016/j.ceramint.2020.03.287.

[16] M. K. Debanath and S. Karmakar, "Study of blueshift of optical band gap in zinc oxide (ZnO) nanoparticles prepared by low-temperature wet chemical method," Mater. Lett., vol. 111, pp. 116–119, 2013, doi: 10.1016/j.matlet.2013.08.069.

[17] D. Kumar, S. K. Jat, P. K. Khanna, N. Vijayan, and S. Banerjee, "Synthesis, characterization, and studies of PVA/Co-doped ZnO nanocomposite films," Int. J. Green Nanotechnol. Biomed., vol. 4, no. 3, pp. 408–416, 2012, doi: 10.1080/19430892.2012.738509.